**XRS**

# A gas proportional-scintillation counter for x-ray spectrometry in the 0.1–3 keV range

## F. I. G. M. Borges,* J. M. F. dos Santos, T. H. V. T. Dias, F. P. Santos and C. A. N. Conde

Departamento de Física da Universidade de Coimbra, 3004-516 Coimbra, Portugal

Results for the energy resolution of a uniform-field gas proportional-scintillation counter are presented for the range 0.1–3 keV. A comparison with results from the literature shows that the detector is most suitable for this energy range. Examples of x-ray fluorescence pulse-height distributions from geological and industrial samples are presented. Copyright © 2004 John Wiley & Sons, Ltd.

## INTRODUCTION

Energy-dispersive x-ray fluorescence (EDXRF) techniques are powerful tools for non-destructive and on-line elemental analysis of materials in industrial environments. Both laboratory and portable systems are currently in use. Standard proportional-ionization counters (commonly known as proportional counters or PCs) are widely used for this purpose, owing to their low cost, large detection areas and room temperature operation. The cooling requirements of semiconductor detectors and the area limitations of Peltier-cooled solid-state devices are often a drawback for industrial applications.

Gas proportional-scintillation counters (GPSC), [the acronym GSPC (gas scintillation proportional counters) is also used in the literature and commonly accepted], which achieve amplification through the production of proportional scintillation, have been widely used in many applications, such as material analysis, medical instrumentation, high-energy physics and astrophysics.[1–3]

In the field of material analysis, GPSCs present significant advantages over proportional counters, since GPSCs operate at room temperature and can have a large detection area with an energy resolution about a factor of two better than a PC.[1–3] In addition, GPSCs do not suffer from space-charge build-up as PCs do when operating under high gain, so GPSCs have an intrinsically high counting rate capability, an advantage for fast analysis applications. In addition, since the amplitude of a GPSC output signal (tenths of volts) is much larger than that of a PC, GPSCs are less prone to electromagnetic and acoustic interference, an important advantage in industrial environments.

Until some years ago, high-performance GPSCs were expensive to build (e.g. ceramic-to-metal joints and large VUV scintillation windows are required), so they were mostly limited to space and high-energy physics applications. However, recent new techniques allow the construction of simple, low-cost, high-performance GPSCs, making them competitive in applications to EDXRF analysis.[2,3]

In this paper, we describe a xenon-filled GPSC suitable for x-ray spectrometry in the 0.1–25 keV range. We pay particular attention to the detector performance for soft x-rays with energies below 3 keV, a region where EDXRF techniques can be used for the analysis of light elements, using an appropriate polyimide radiation window. In this low-energy region, the energy resolution of GPSCs will approach and become similar to large area solid-state detectors, e.g. the HP-Ge detector.[4] In addition, the use of a gas detection medium allows x-ray interactions to occur at larger distances from the front electrode, reducing the low-energy tails caused by the loss of primary electrons to this electrode.[5,6] Examples of x-ray fluorescence pulse-height distributions from geological and industrial samples are presented.

## RESULTS AND DISCUSSION

### Experimental set-up

The GPSC used in the present work is shown schematically in Fig. 1. A description of the basic set-up and GPSC operation principles can be found elsewhere.[2,3] The present GPSC has a 6 mm diameter polyimide window with ~30% transmission down to 250 eV (PG-W from Metorex, Finland). The absorption and scintillation regions are 2.2 and 1 cm long, respectively, and the detector was filled with pure Xe at 800 Torr (1 Torr = 133.3 Pa). The detector gas filling is continuously purified by convection using non-evaporable getters (SAES Model St 707 getters) maintained at a temperature of about 180 °C, allowing the detector to work for several months with the same gas without contamination problems. The reduced electric fields in the drift and scintillation regions are 0.3 and 5.5 V cm$^{-1}$ Torr$^{-1}$, respectively. The scintillation is collected by an EMI 9266 MgF$_2$ photomultiplier, and the signal from the anode is amplified using a Canberra Model 2005 preamplifier and an Ortec 570 linear amplifier with 10 μs shaping time constants. The amplified signal is collected by a Nucleus PCAII multi-channel analyzer. The high voltages polarizing the GPSC grids were

*Correspondence to: F. I. G. M. Borges, Departamento de Física da Universidade de Coimbra, Rua Larga, 3004-516 Coimbra, Portugal.
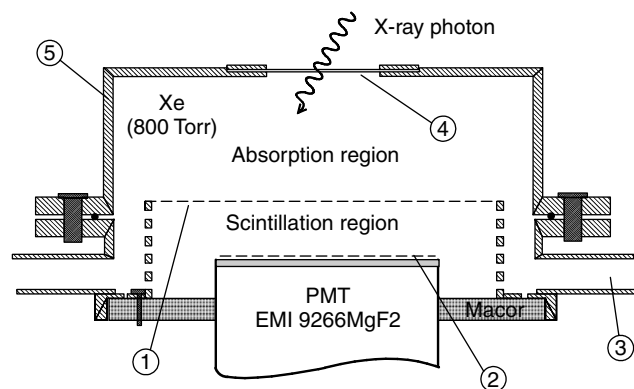E-mail: fborges@gian.fis.uc.pt

**Figure 1.** Schematic diagram of the GPSC: 1, first grid; 2, second grid; 3, gas outlet to purifier; 4, entrance window; 5, stainless-steel enclosure.

taken from HP6110A and Fast NHQ206L power supplies, with peak-to-peak ripple noise below 2 mV.

### Energy resolution and linearity

Different x-ray energies $E_{xr}$ were generated by exciting the fluorescence lines of various targets with $\alpha$-particles from a $^{244}$Cm source or x-rays from a $^{55}$Fe source. The energy spectra were fitted to Gaussian distributions over a linear background by a least-squares method.

Figure 2 depicts the energy resolution $R$ obtained as $R = H/c$, where $H$ is the full width at half-maximum and $c$ is the position of the centroid of the Gaussian fittings to the measured spectra. Also represented are the experimental data from the literature.[4,6–9] In the energy range considered, and apart from the results from Simons and de Korte,[8] $R$ of the present GPSC is found to be better than for the competitive detectors, including the HP-Ge detector for $E_{xr}$ below 500 eV. Note that the GPSC is simpler to build, may have larger window areas and involves less demanding operating requirements. In addition, our GPSC offers good
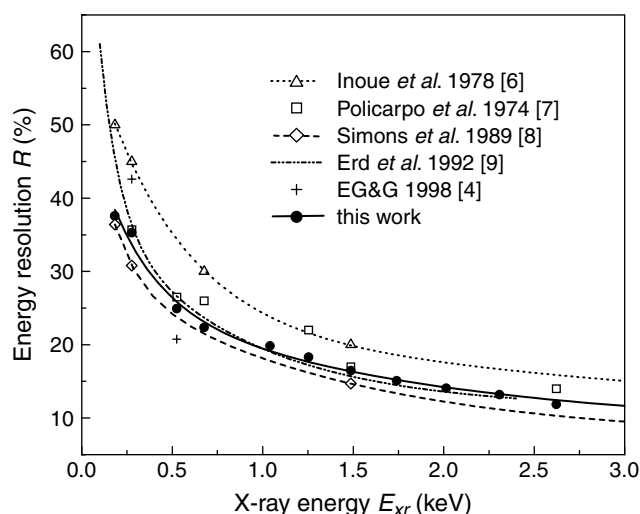
**Table 1.** Energy resolution obtained with the present GPSC for the $K_\alpha$ fluorescence lines $E_{xr}$ from various elements, (the Xe M photoionization edges are also indicated)

| Element or Xe edge | $E_{xr}$ (eV) or Xe edge (eV) | $R$ (%) |
|---|---|---|
| B | 183 | 37.6 |
| C | 277 | 35.3 |
| O | 525 | 24.9 |
| F | 677 | 22.4 |
| $M_{4,5}$ | 683 | |
| $M_{2,3}$ | 972 | |
| Na | 1041 | 19.9 |
| $M_1$ | 1148 | |
| Mg | 1254 | 18.3 |
| Al | 1487 | 16.5 |
| Si | 1740 | 15.1 |
| P | 2014 | 14.1 |
| S | 2308 | 13.2 |
| Cl | 2622 | 11.9 |
| Ti | 4510 | 9.2 |
| Mn | 5895 | 8.4 |
| Ag | 22100 | 5.0 |

energy resolution up to 22 keV, as shown in Table 1, where all results are summarized.

In Fig. 3, the results for the position of the pulse-height distribution centroids are plotted as a function of $E_{xr}$. We observe that the behaviour is linear, apart from a small discontinuity at the Xe M-edges that the present GPSC was able to detect, as discussed in an earlier paper.[10]

The detection efficiency of the detector for fully absorbed, collimated x-rays is shown in Fig. 4 as a function of x-ray energy. The efficiency values were calculated considering losses of primary electrons due to backscattering to the detector entrance window[11] and losses of incident x-ray photons, which at low energies may be absorbed by the window,[12] and at higher energies ($E_{xr}$ above ~10 keV) may travel through the detector absorption region without being absorbed.[13] The escape of the Xe L fluorescence was taken into account and considered to represent a loss of 5% from the full-energy peak (the Xe L fluorescence yield is ~10%,[14] and escape is half this value at most).

In the low-energy region $E_{xr} < 3$ keV, the photon and electron losses to the window are the mechanisms responsible for the general shape of the efficiency curve. The observed multiple abrupt drops in the efficiency curve reflect either some photon absorption at the absorption edges of the polyimide window components, or losses due to increased backscattering of electrons when $E_{xr}$ falls near the Xe edges. The data concerning this last effect were taken from a previous Monte Carlo simulation of the absorption of x-rays in Xe.[11]

### Sample analysis

Figures 5–7 show the energy spectra from quartz, andalusite and feldspar targets excited with both $\alpha$ and x-ray sources. The window-to-sample distance is 10 mm in all cases.
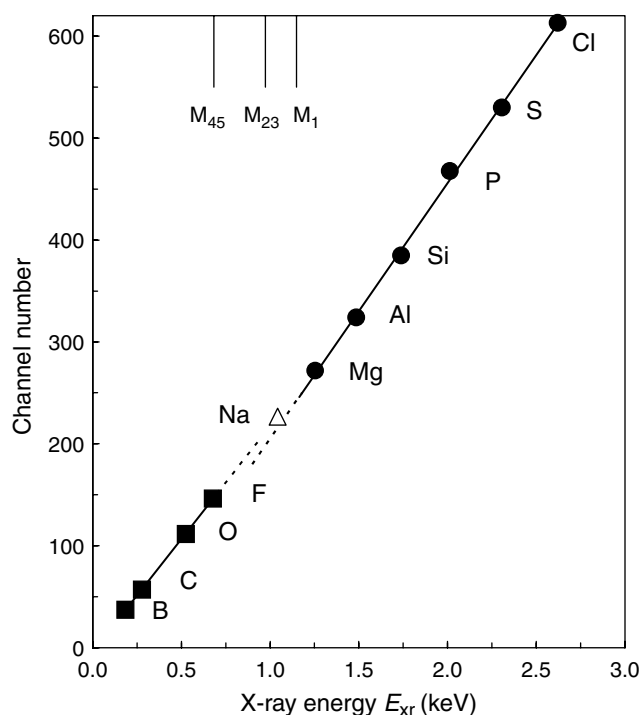


**Figure 2.** Energy resolution of the present GPSC as a function of $E_{xr}$, compared with other measurements: uniform field GPSC;[6] spherical anode GPSC;[7] uniform field, driftless GPSC;[8,9] HP-Ge detector.[4]

**Figure 3.** Channel number for the peaks in the energy spectra obtained with the present GPSC, corresponding to the $K_\alpha$ lines of various elements. The vertical lines indicate the Xe M-edges.
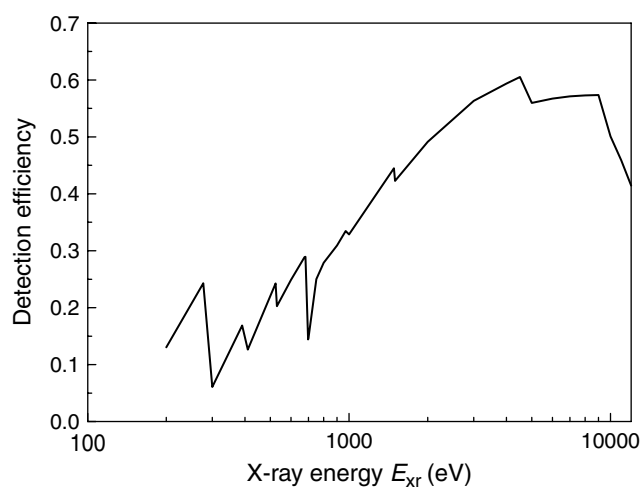


**Figure 4.** Calculated detection efficiency of the Xe-filled GPSC as a function of x-ray energy.

In Fig. 5, three peaks are clearly distinguishable. The first, above the electronic noise (which appears only below 100 eV), belongs to the carbon $K_\alpha$ line (277 eV), and is due to the excitation of C in the polyimide window by backscattered $\alpha$-particles. The second and third peaks correspond to the O (525 eV) and Si (1740 eV) $K_\alpha$ lines from the excited quartz target.

Figure 6 shows the spectra obtained by exciting an andalusite sample with both a $^{244}$Cm $\alpha$-source (gray line) and an $^{55}$Fe x-ray source (black line). We observe several peaks from C to Mn $K_\alpha$ lines. The O, Al, and Si $K_\alpha$ lines (525, 1487 and 1740 eV, respectively) are clearly distinguishable and belong to the sample. The carbon $K_\alpha$ line is again due
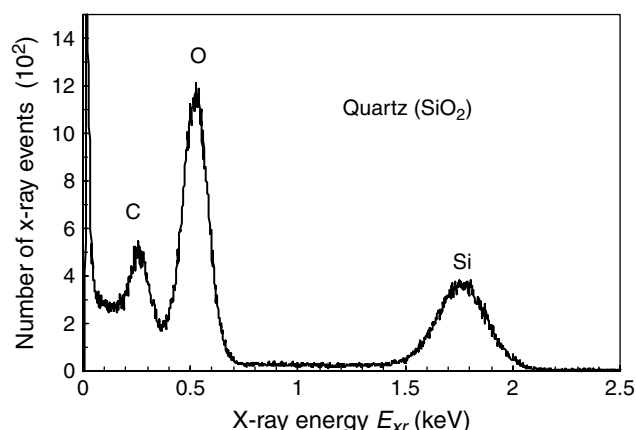


**Figure 5.** Energy spectrum obtained with the present GPSC by exciting an SiO$_2$ sample with $\alpha$-particles from a $^{244}$Cm source.
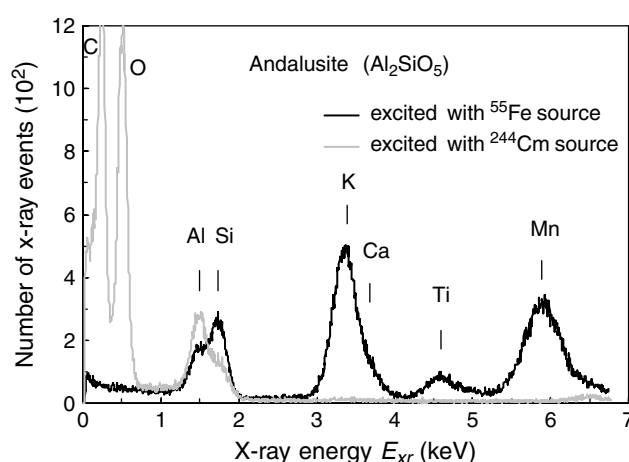


**Figure 6.** Energy spectrum obtained with the present GPSC by exciting an andalusite sample with $\alpha$-particles from a $^{244}$Cm source (gray line) and with x-rays from a $^{55}$Fe source (black line).
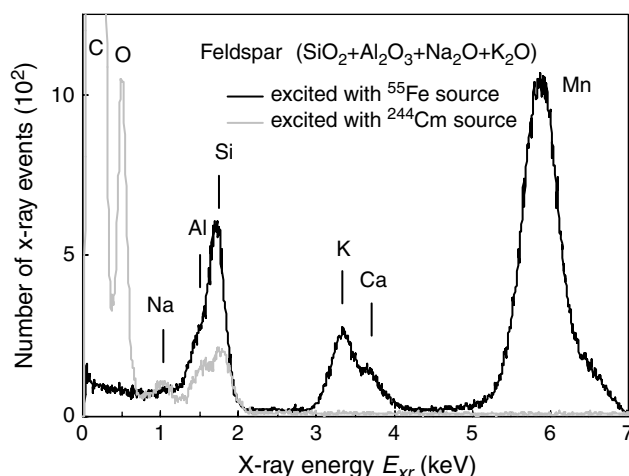


**Figure 7.** Energy spectrum obtained with the present GPSC by exciting a feldspar sample with $\alpha$-particles from a $^{244}$Cm source (gray line) and with x-rays from a $^{55}$Fe source (black line).

to the presence of C in the detector window; the Mn line corresponds to some backscattered x-rays from the $^{55}$Fe source. The other peaks belong to impurities in the sample.

In Fig. 7, we observe the two spectra obtained by exciting feldspar with both the $\alpha$ (gray line) and x-ray (black line) sources. The C and Mn K$_\alpha$ lines appear for the reasons mentioned above. In addition, we can observe the O, Na, Al, Si, K and Ca K$_\alpha$ lines (525, 1041, 1487, 1740, 3314 and 3690 eV, respectively) from the feldspar sample.

## CONCLUSIONS

A uniform-field gas proportional-scintillation counter is described and the results for its energy resolution are presented and compared with results from different gas and semiconductor detectors, with special attention to the 0.1–3 keV x-ray energy range. In this energy range, the energy resolution of the GPSC is found to be comparable to that of driftless detectors (usually considered the best solution for this range), better than that of previously developed uniform-field and spherical anode GPSC detectors for soft x-rays, and even better than that of the HP-Ge detector for energies below 500 eV. In addition, the GPSC is simple to build, may have large window areas and involves less demanding electronics and operating requirements than solid-state or driftless gas scintillation counters, also providing good performance over a wide energy range (up to 25 keV).

## REFERENCES

1. Knoll GF. *Radiation Detection and Measurement*, (3rd edn). Wiley: New York, 2000.
2. Dias THVT. *NATO ASI Ser. B Phys.* 1994; **326**: 543.
3. dos Santos JMF, Lopes JAM, Veloso JFCA, Simões PCPS, Dias THVT, Santos FP, Rachinhas PJBM, Ferreira LFR, Conde CAN. *X-Ray Spectrum.* 2001; **30**: 373.
4. *Modular Pulse Processing Electronics and Semiconductor Radiation Detectors*. EG&G Catalog 97/98. Princeton, NJ: EG&G Princeton Applied Research, 1997–98; 1.80, 1.81.
5. Dias THVT, Santos FP, Stauffer AD, Conde CAN. *Phys. Rev. A* 1992; **46**: 237.
6. Inoue H, Koyama K, Matsuoka M, Ohashi T, Tanaka Y, Tsunemi H. *Nucl. Instrum. Methods* 1978; **157**: 295.
7. Policarpo AJPL, Alves MAF, Salete M, Leite SCP, dos Santos MCM. *Nucl. Instrum. Methods* 1974; **118**: 221.
8. Simons DG, de Korte PAJ. *Nucl. Instrum. Methods Phys. Res. A* 1989; **277**: 642.
9. Erd C, Bavdaz M. *Internal Publication ESLAB 92/094.* Noordwijk: ESTEC: 1992.
10. Borges FIGM, Dias THVT, Santos FP, Rachinhas PJBM, dos Santos JMF, Conde CAN. *Nucl. Instrum. Methods Phys. Res. A* 2003; **505**: 242.
11. Borges FIGM, Santos FP, Dias THVT, Rachinhas PJBM, Conde CAN, Stauffer AD. *IEEE Trans. Nucl. Sci.* 2002; **49**: 917.
12. http://www.metorex.fi/pages/space_products/windows.htm.
13. http://www-cxro.lbl.gov/optical_constants/gastrn2.html.
14. http://epmalab.uoregon.edu/UCB_EPMA/fluoresc.htm.